Solution structure of a 2:1 quindoline–c-MYC G-quadruplex: insights into G-quadruplex-interactive small molecule drug design

Jixun Dai [‡], Megan Carver [‡], Laurence H. Hurley[‡§‖†], Danzhou Yang[‡§‖†*]

Supplementary Information

Table S1. Proton chemical shifts for the 2:1 quindoline-Pu22 complex at 35 °C [a].

MycG4	H6/H8	H2/H5/Me	H1'	H2'/H2"	H3'	H4'	H5'/H5"	NH1/NH3
T4	7.06	1.53	5.64	1.32,1.80	4.29	3.67	3.34	
G5	7.06		5.26	2.03,1.87	4.54	3.92	3.57,3.65	
A6	8.14	8.06	6.30	2.68,2.78	4.96	4.23	3.87,3.93	
G7	8.07		6.05	2.75,2.99	5.00	4.50	4.17,4.23	11.41
G8	7.66		6.09	2.62,2.91	5.01	4.51	4.31,4.29	10.89
G9	7.64		6.31	2.78,2.70	5.18	4.60	4.32,4.36	10.51
T10	7.87	2.00	6.51	2.47,2.67	5.10	4.58	4.28,4.34	10.27
G11	7.86		6.02	2.38,2.84	5.06	4.47	4.29,4.31	11.02
G12	7.72		6.00	2.56,2.77	5.01	4.43	4.19,4.24	11.08
G13	7.68		6.32	2.75,2.68	5.07	4.47	4.26	10.88
T14	7.67	1.95	6.25	2.24,2.48	4.74	3.96	3.82	
A15	8.55	8.36	6.66	3.07,2.95	5.19	4.59	4.20,4.30	
G16	7.97		6.08	2.55,2.90	5.01	4.51	4.23,4.29	11.08
G17	7.61		6.10	2.60,2.92	5.00	4.53	4.20,4.25	10.90
G18	7.70		6.36	2.76,2.69	5.16	4.60	4.29,4.34	10.56
T19	7.88	2.01	6.52	2.48,2.68	5.11	4.60	4.28,4.35	
G20	7.83		6.00	2.34,2.79	5.07	4.48	4.28,4.33	11.09
G21	7.79		5.98	2.64,2.71	5.06	4.52	4.20,4.28	11.13
G22	7.60		6.22	2.66,2.73	5.09	4.54	4.27,4.32	10.67
T23	7.52	1.85	6.01	2.00,2.32	4.81	4.28	4.12,4.24	
A24	7.79	7.43	5.52	2.04,2.20	4.56	3.81	3.82	
A25	7.78	7.58	5.78	2.27,2.17	4.39	3.85	3.69,3.77	

Qui [b]	H1'	H2'	H4'	Me5'	H2	H3	H4	H5	H8	H9	H10	H11
	4.05	3.42	3.21	1.20	7.23	7.18	6.91	7.56	6.96	7.01	6.66	7.55

a). The chemical shifts are measured in 10 mM K-phosphate , pH 6.0 at 35 °C and referenced to DSS.
b). Proton resonances between the two quindoline molecules are not resolved.

Figure S1. Imino proton regions of the 1D ^{1}H NMR titration spectra of the wild-type mycPu22 with quindoline in pH7 100 mM K^+ solution. The imino region of 1D ^{1}H NMR spectrum of the 2:1 complex of quindoline with the Pu22 sequence is shown at the bottom for comparison.

Figure S2. The imino proton region with assignment of the 1D ^{1}H NMR spectrum of the 2:1 quindoline:MycG4 complex in pH7 100 mM K^+ solution (top), and imino proton assignments using 1D ^{15}N-filtered experiments on 2:1 quindoline:DNA complexes of site-specific labeled Pu22 oligonucleotides.

Figure S3. (A) The expanded H8/H6-H1′ region of the 2D-NOESY spectrum of the 2:1 quindoline:MycG4 complex in pH7 100 mM K^+ solution at 30°C. The sequential assignment pathway is shown except for the 3'-T(23)A(24)A(25). The NOE peaks related with the multiple conformations of the 3'-end are shown in the red box.

Figure S4. The expanded quindoline aromatic-aromatic region of the 2D-NOESY spectrum of the 2:1 quindoline:MycG4 complex in pH7 100 mM K^+ solution at 30°C (A) and in pH6 10 mM K^+ solution (B) at 35°C.

Figure S5. The expanded methyl/H2'/H2'' region of the 2D-NOESY spectrum of the 2:1 quindoline:MycG4 complex in pH7 100 mM K^+ solution at 30°C. Minor peaks are observed for quindoline Me5' and H4' protons (labeled with asterisks). Exchange NOE peaks are clearly observed between the major and minor peaks, and are labeled by red arrows.

Figure S6. The expanded H8/H6-H3′/H4′ region of the 2D-NOESY spectrum of the 2:1 quindoline:MycG4 complex in pH6 10 mM K^+ solution at 35°C. The inter-residue NOEs of MycG4 at G5-A6-G7 and G22-T23 steps are labeled.

Figure S7. The imino proton regions of hydrogen-deuterium exchange experiments of MycG4 (A) and 2:1 Quindoline:MycG4 complex (B) at 25°C in pH6 10 mM K^+ solution. As indicated by the

imino protons from the middle G-tetrad, the $t_{½}$ of hydrogen-deuterium exchange is about 12 days for the 2:1 Quindoline:MycG4 complex compared to 2 days for the free MycG4. The freeze-dried sample was dissolved into 99.9% D2O to start the hydrogen-deuterium exchange. d is labeled for day, h for hour, and m for minute. The experimental dead time is about 5 min. Each spectrum was collected with the number of scans of 64.

Figure S8. The NMR molecular structure of the free MycG4 formed in Pu22 in K^+ solution (PDB ID 1XAV). A25 folds back to form a potential base pair with T23 to cover the bottom G-tetrad, while A24 stays above the T23:A25 base pair**.**

Figure S9. The side and top view of the 2:1 quindoline-MycG4 complex structure with a wild-type G23 from molecular dynamics (MD) simulation calculation. To generate the initial structure, the T23 of MycG4 was substituted to the wild-type G23 in the NMR structure of the 2:1 quindoline-MycG4 complex using InsightII Biopolymer module. 10 ps of MD simulation with time steps of 1fs at 300K in explicit solvents was performed using Insight II/Discover with CFF forcefield. Two K^+ ions were included between the three G-tetrad planes, and 21 K^+ ions were used to counter the negative charges of DNA backbone. The lowest energy conformation from MD simulation trajectory was further energy-minimized to get the final structure. A potential hydrogen bond between quindoline N1H and G23O6 is shown as a dashed line.

Figure S10. Imino proton regions of the 1D ^{1}H NMR spectra of the free (top) and 2:1 quindoline complexes (bottom) of various modified c-MYC promoter sequences in pH 7 100 mM K^+ solution at 25 °C. The modified sequences are shown above the spectra.

Figure S11. Surface potential visualization of the 5'-face and 3'-face of c-Myc G-quadruplex in the 2:1 quindoline:MycG4 complex, with the 5'-end view (top left), 3'-end view (top right), and two side views (bottom).

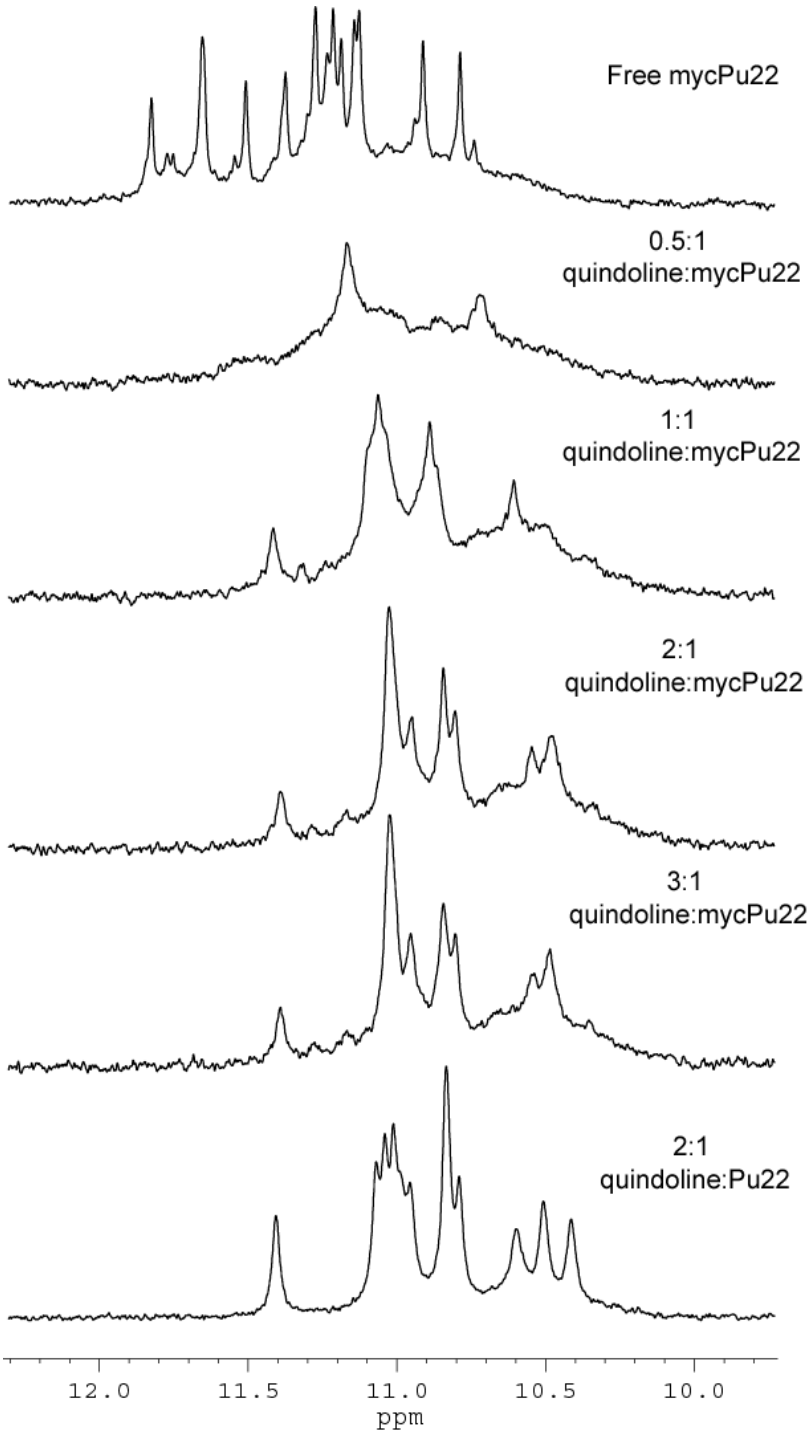
Free mycPu22
0.5:1
quindoline:mycPu22
1:1
quindoline:mycPu22
2:1
quindoline:mycPu22
3:1
quindoline:mycPu22
2:1
quindoline:Pu22
12.0
11.5
11.0
10.5
10.0
ppm

Fig S1.

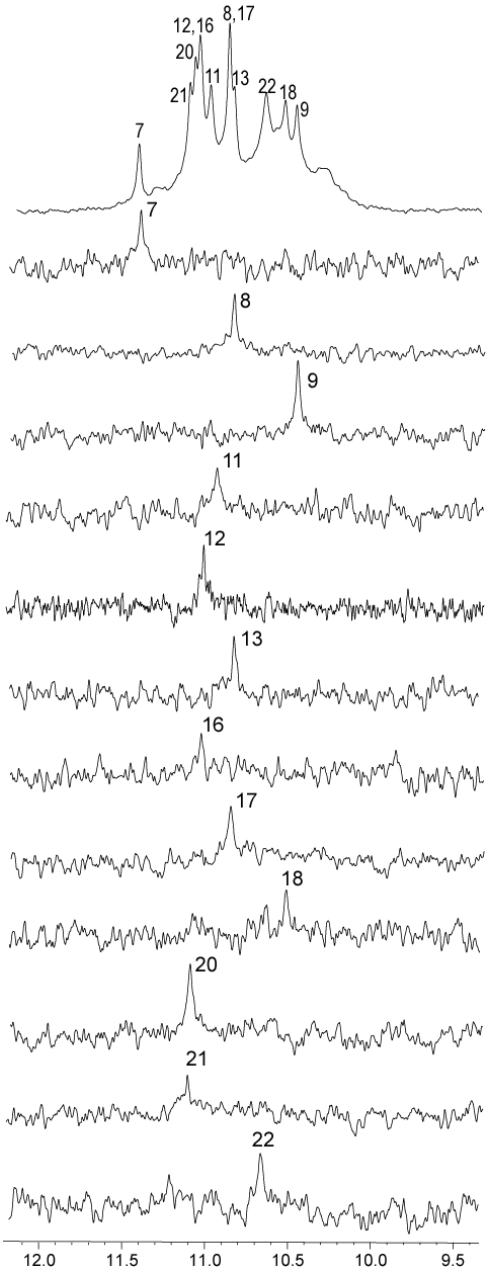
12,16
8,17
20
11
13
21
22
18
9
7
7
8
9
11
12
13
16
17
18
20
21
22
12.0
11.5
11.0
10.5
10.0
9.5

Fig S2.

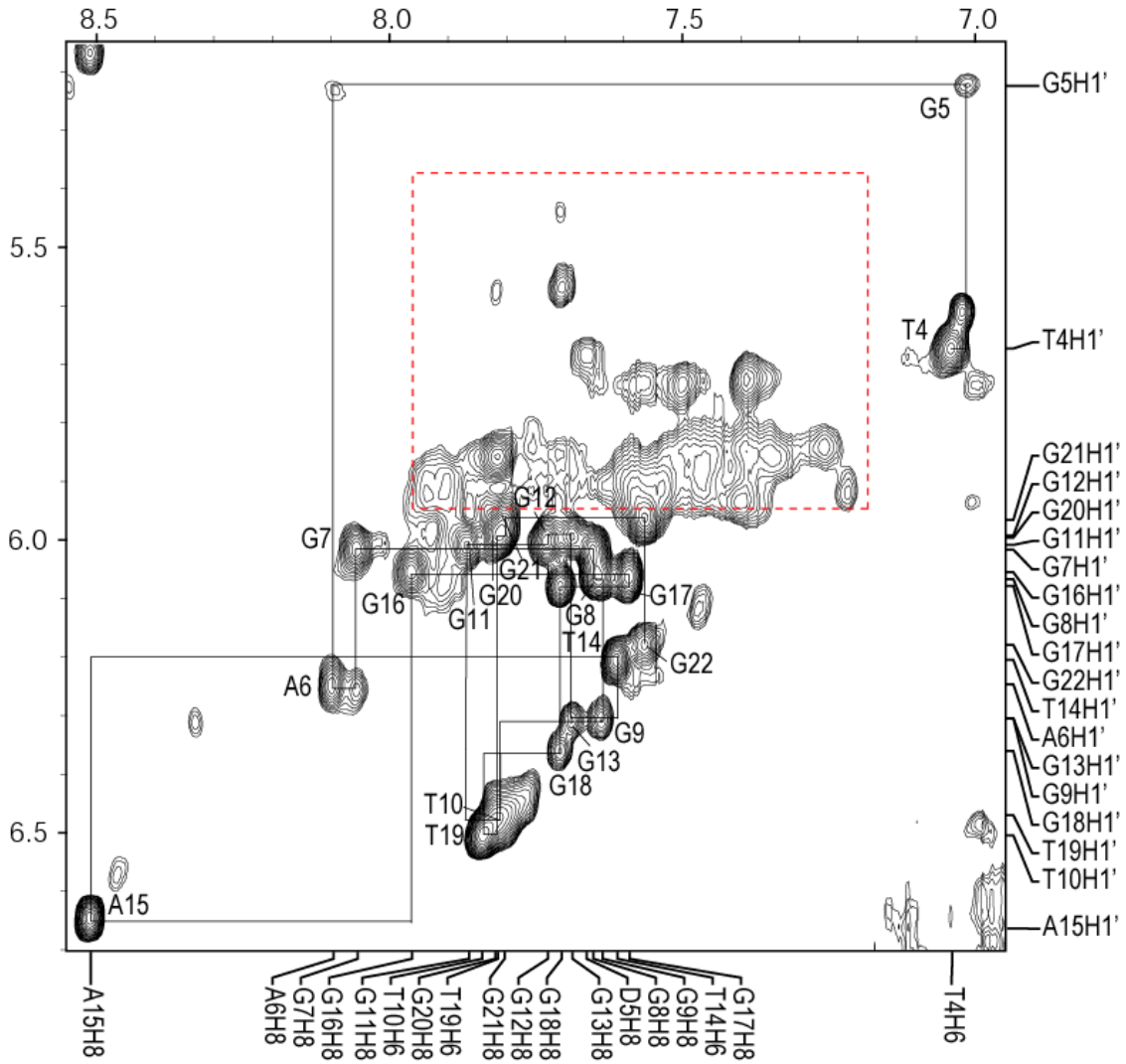
8.5
8.0
7.5
7.0
5.5
6.0
6.5
G5H1'
G5
T4
T4H1'
G21H1'
G12H1'
G20H1'
G11H1'
G7H1'
G16H1'
G8H1'
G17H1'
G22H1'
T14H1'
A6H1'
G13H1'
G9H1'
G18H1'
T19H1'
T10H1'
A15H1'
G12
G7
G21
G16
G20
G11
G8
G17
T14
G22
A6
G9
G13
G18
T10
T19
A15
A15H8
A6H8
G7H8
G16H8
G11H8
T10H6
G20H8
T19H6
G21H8
G12H8
G18H8
G13H8
D5H8
G8H8
G9H8
T14H6
G17H8
T4H6

Fig S3.

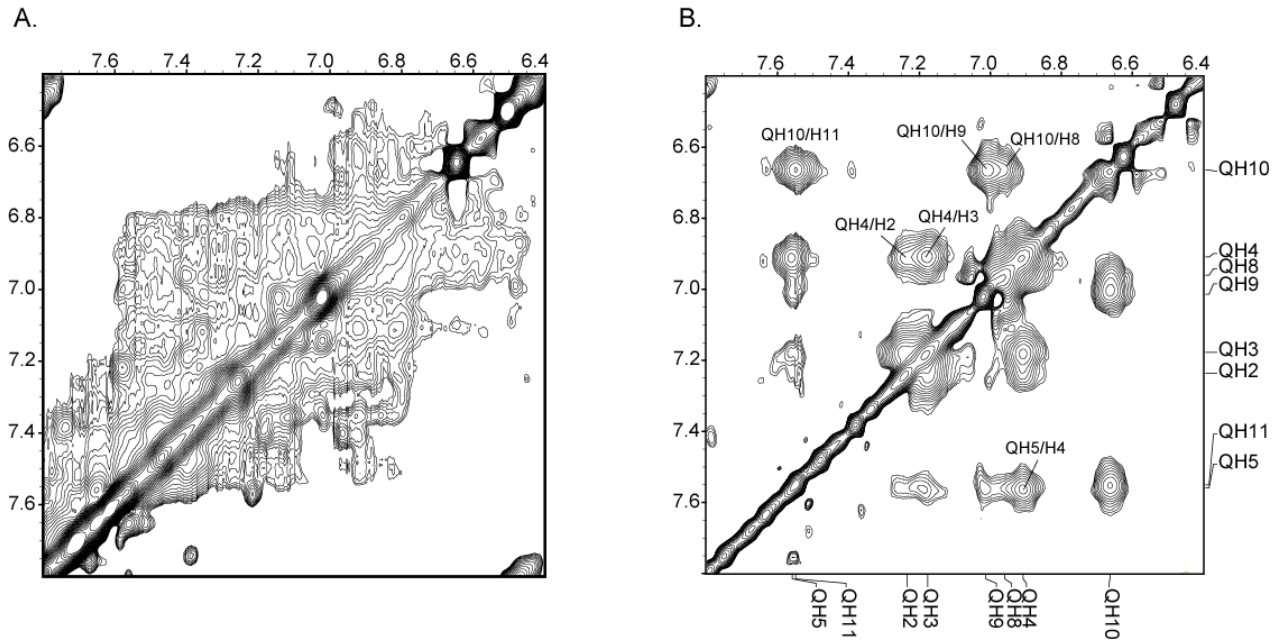
A.
B.
7.6
7.4
7.2
7.0
6.8
6.6
6.4
QH10/H11
QH10/H9
QH10/H8
QH4/H2
QH4/H3
QH5/H4
QH10
QH4
QH8
QH9
QH3
QH2
QH11
QH5

Fig S4.

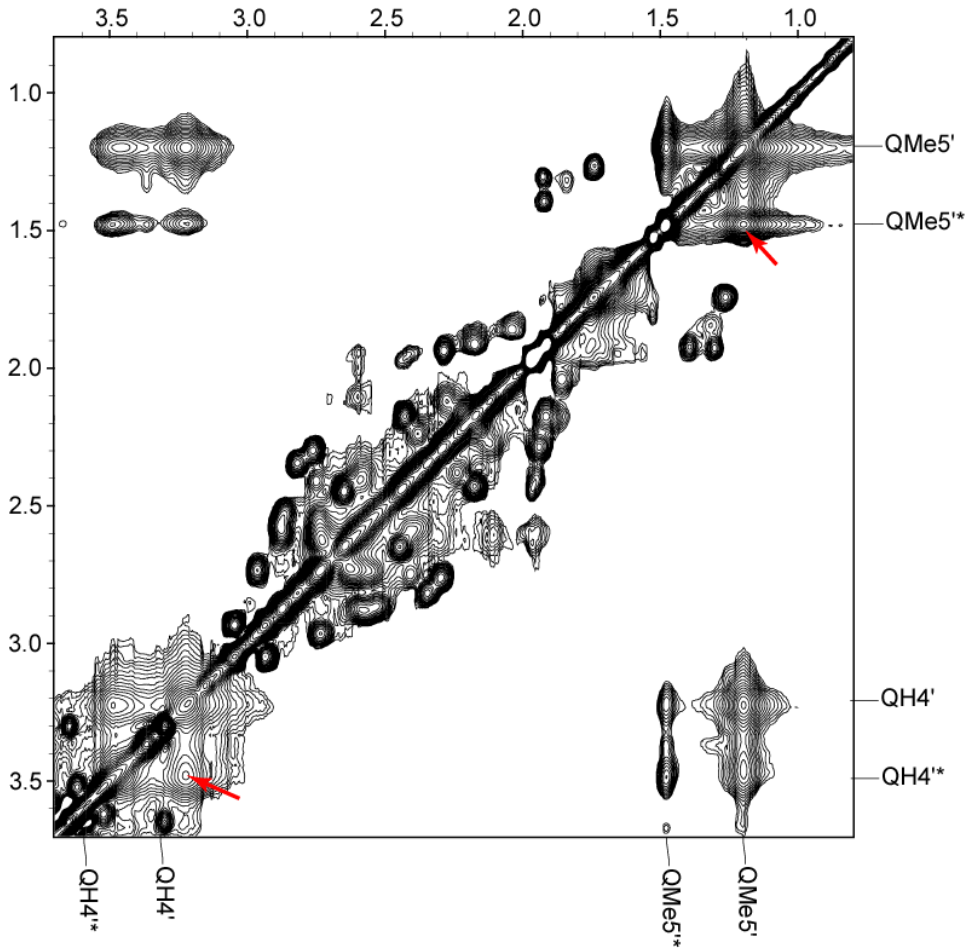
3.5
3.0
2.5
2.0
1.5
1.0
1.0
1.5
2.0
2.5
3.0
3.5
QMe5'
QMe5'*
QH4'
QH4'*
QH4'*
QH4'
QMe5'*
QMe5'

Fig S5.

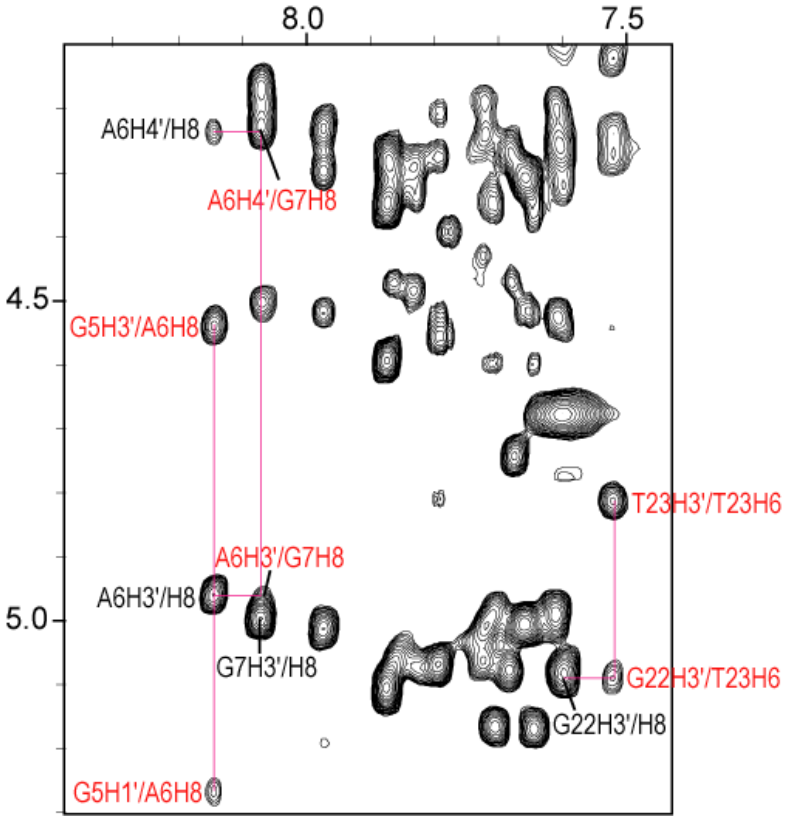
8.0
7.5
4.5
5.0
A6H4'/H8
A6H4'/G7H8
G5H3'/A6H8
T23H3'/T23H6
A6H3'/G7H8
A6H3'/H8
G7H3'/H8
G22H3'/T23H6
G22H3'/H8
G5H1'/A6H8

Fig S6.

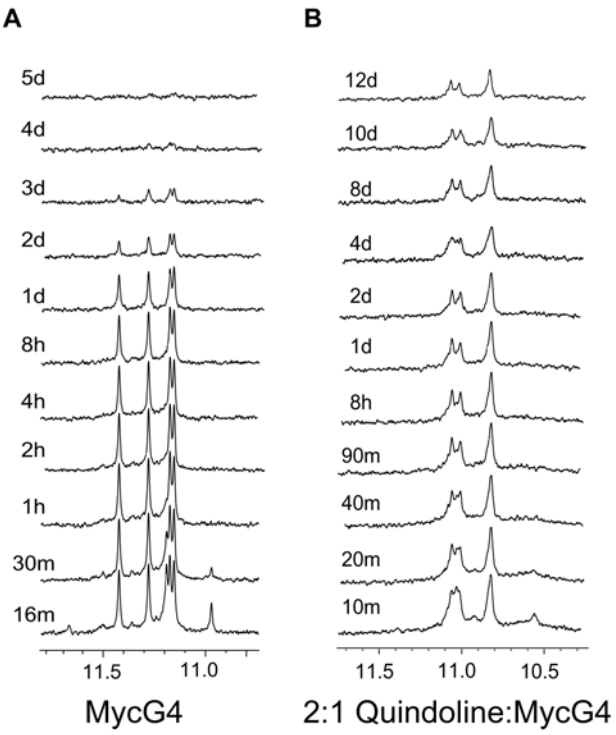
A
B
5d
4d
3d
2d
1d
8h
4h
2h
1h
30m
16m
11.5
11.0
MycG4
12d
10d
8d
4d
2d
1d
8h
90m
40m
20m
10m
11.5
11.0
10.5
2:1 Quindoline:MycG4

Fig S7.

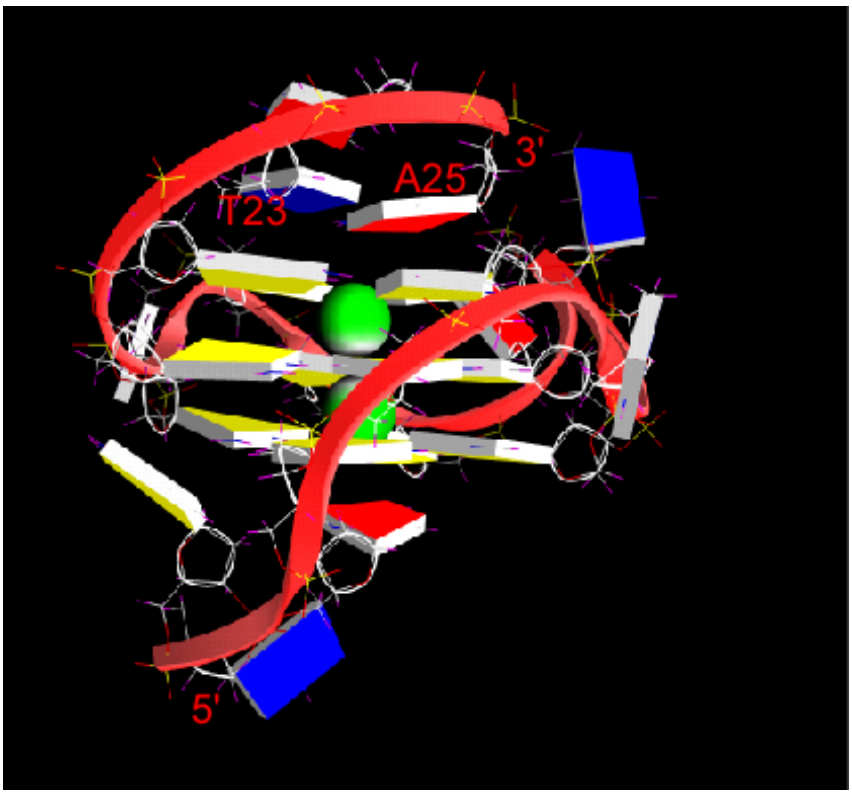

Fig S8.

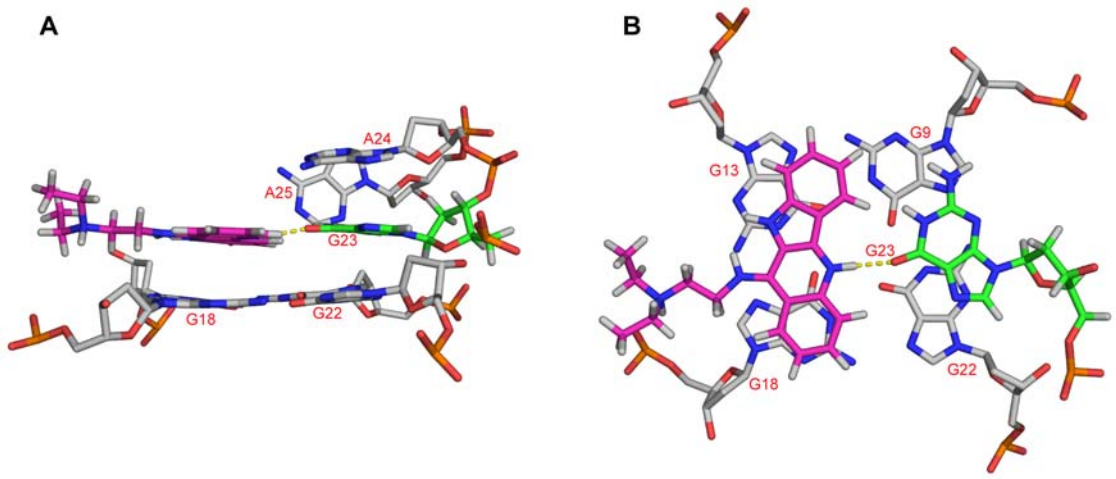

Fig S9.

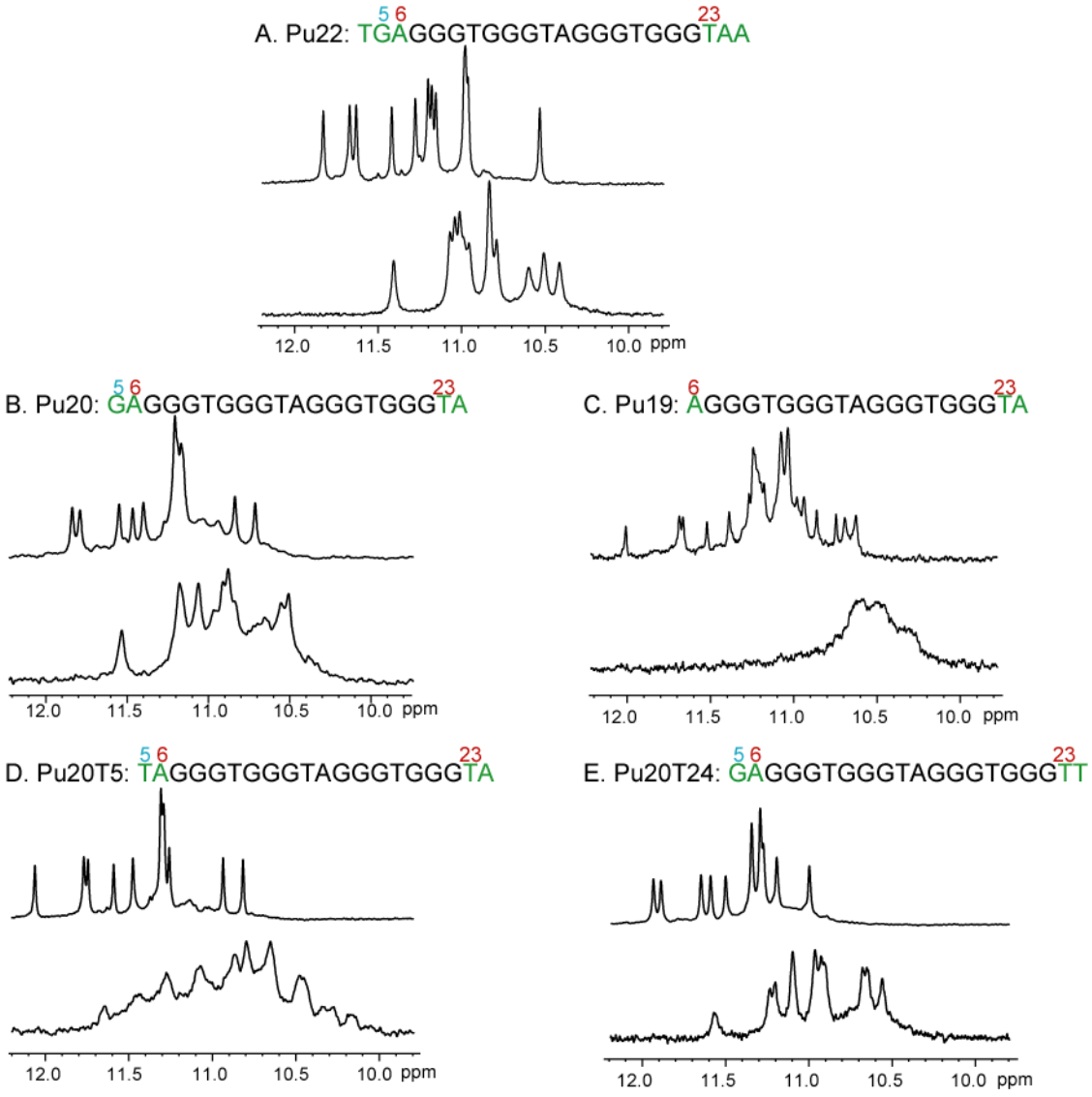
A. Pu22: TGAGGGTGGGTAGGGTGGGTAA
5 6
23
12.0 11.5 11.0 10.5 10.0 ppm
B. Pu20: GAGGGTGGGTAGGGTGGGTA
5 6
23
12.0 11.5 11.0 10.5 10.0 ppm
C. Pu19: AGGGTGGGTAGGGTGGGTA
6
23
12.0 11.5 11.0 10.5 10.0 ppm
D. Pu20T5: TAGGGTGGGTAGGGTGGGTA
5 6
23
12.0 11.5 11.0 10.5 10.0 ppm
E. Pu20T24: GAGGGTGGGTAGGGTGGGTT
5 6
23
12.0 11.5 11.0 10.5 10.0 ppm

Fig S10.

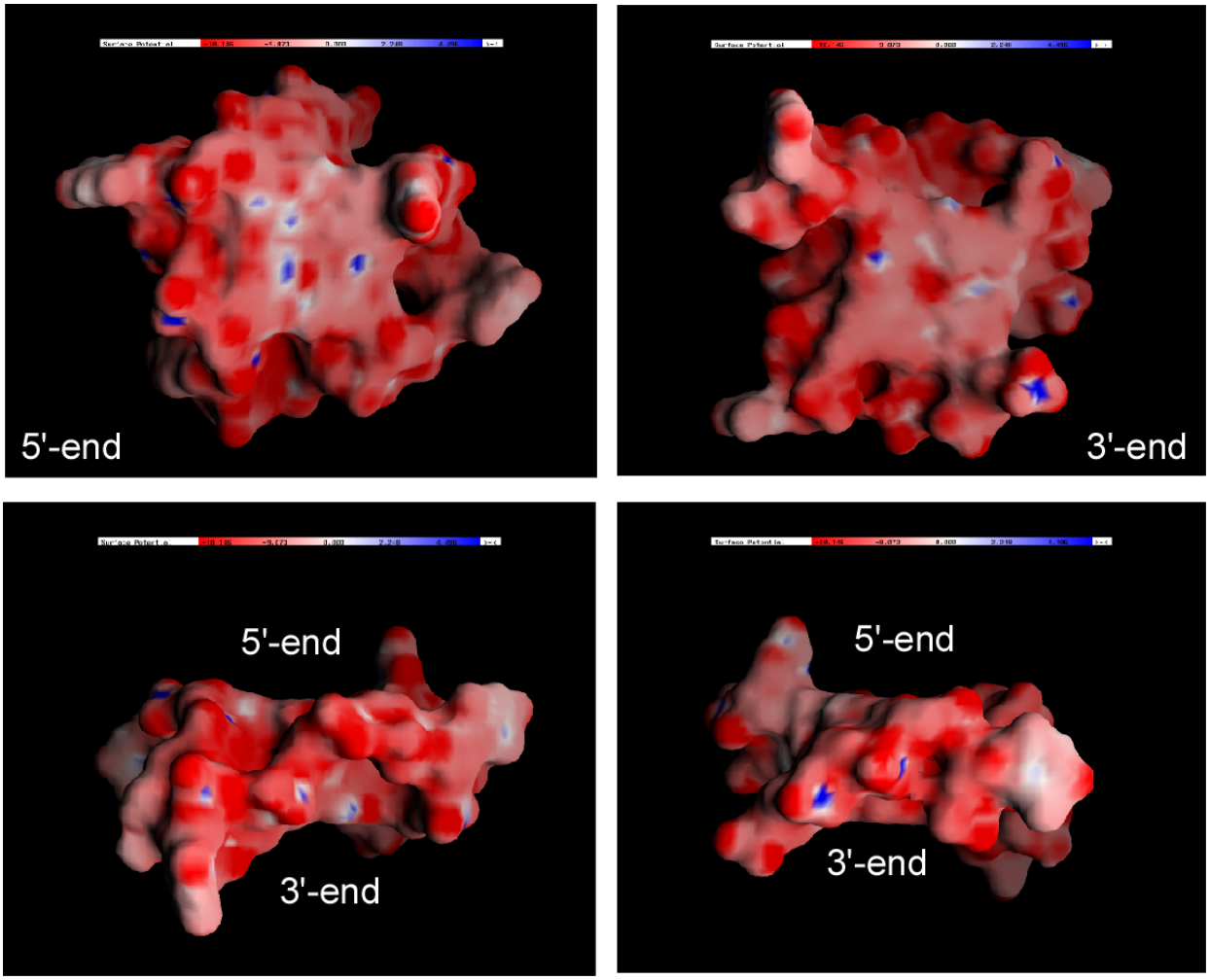

Fig S11.